FORMATION OF THE BANDED TERRAIN OF HELLAS PLANITIA, MARS.

C. W. Cook[1], S. Byrne[1], and M. M. Sori[2], [1]Lunar and Planetary Laboratory, University of Arizona, Tucson, AZ 85721 (clairec@lpl.arizona.edu), [2]Purdue University

Introduction: The extent of past glaciation on Mars is an important unknown in determining its water inventory and climate history. Understanding the origin of the banded terrain in Hellas basin could shed light on this aspect of martian history. Banded terrain is a surface morphology, ~1.9–3.7 Gyr old, composed of bands with linear, lobate, and circular forms found primarily in northwest Hellas (Fig. 1 a–c) [1, 2]. Linear bands are typically ~5 km long, 300 m wide, and 10 m in relief [2]. In some locations, banded terrain superposes honeycomb terrain, which is made up of adjacent ~10 km wide depressions [3] (Fig. 1 d).

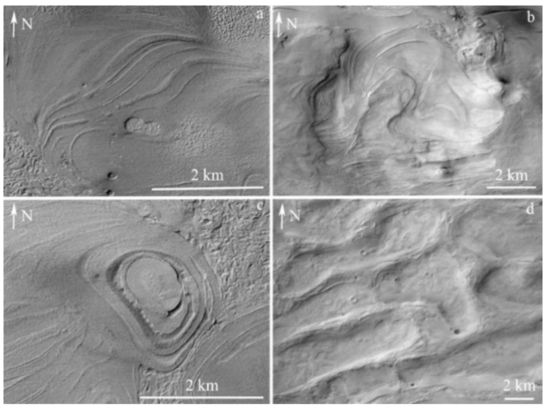

Figure 1: Examples of a) linear banded terrain, b) lobate banded terrain, c) circular banded terrain, and d) honeycomb terrain. CTX image D21_035353_1431.

Bands starting at topographic highs and appearing to flow downslope led Diot et. al. [2, 4] to suggest banded terrain was due to gravity driven viscous flow of a thin ice-rich layer. More comprehensive measurements by Bernhardt et al. [1] suggested that band orientation does not always correlate with local slopes. They hypothesized that small-scale stresses resulting from a thick ice sheet may have deformed subglacial sediment. Terrestrial ribbed bedforms, ridges found over large areas of past ice sheets [5], may have formed by flow of ice and subglacial sediment [6, 7]. These can exist at a similar scale to banded terrain [5] but their morphology differs, challenging their interpretation as an analogue.

Here, we perform quantitative modeling to test the hypothesis that banded terrain may be formed by subglacial till deformation. Results that would support this hypothesis include 1) peak basal velocities in a Hellas ice sheet aligned with banded terrain and 2) reproducing banded terrain relief, scale, and shape.

Methods: Ice and subglacial till deformation are simulated using the finite element modeling software COMSOL. The model consists of two parts. One part is a large-scale, low-resolution model of an ice sheet in Hellas, used to find the velocity at the boundary between the base of the ice sheet and the top of the till layer. The second part is a small-scale, high-resolution model of subglacial till with a surface velocity prescribed as a boundary condition based on the ice sheet model results.

Ice rheology is modeled using a viscous flow law: $\dot{\varepsilon} = Ae^{-2n\varphi}e^{-Q/RT}\tau_E^{\,n-1}\tau d^{-p}$ where $\dot{\varepsilon}$ is the strain rate, A is a material parameter, n is the stress exponent, φ is the dust volume fraction, Q is activation energy, R is the gas constant, T is temperature, τ_E is the effective stress, τ is the deviatoric stress, d is the grain size, and p is the grain size exponent [8]. We combine strain rates from dislocation creep, grain boundary sliding, and basal slip deformation mechanisms, with different parameters for these three modes [8]. Till rheology is modeled using a similar viscous flow law (as in [9]) of the form: $\dot{\varepsilon} = B^{-m}\tau_E^{\,m-1}\tau$ where B is the hardness factor (related to viscosity) and m is the stress exponent.

The parameters to be varied for the ice sheet model are ice and till thickness, surface temperature, basal heat flux, till rheology parameters, and dust content. For initial tests, the surface of the ice sheet is a paraboloid centered at some location in Hellas, but future models will use an ice surface based on accumulation rates from GCMs [e.g., 10]. The till thickness is based on banded terrain relief measurements (10–30 m) [1, 2]. Surface temperatures will be calculated for a range of obliquities using a thermal model. Heat flux is varied between present day estimates (15–30 mW/m^2) [11, 12] and higher values inferred for the Noachian-Hesperian boundary (~60 mW/m^2) [13]. The till viscosity ranges between a measured value for terrestrial till (~3×10^{12} Pa s) [14] and a higher value that may be more appropriate to colder till on Mars (~8×10^{14} Pa s). Till has been described as having a moderately nonlinear viscous behavior in some studies, corresponding to a small value of the stress exponent (~3), but as nearly plastic in other studies, corresponding to a large value of the stress exponent (~40) [9], so both end-member behaviors will be modeled by varying this parameter. The dust content of the ice will be varied based on the low dust contents inferred from observations of mid-latitude ice (1–10%) [e.g., 15, 16] and higher values suggested by GCM results [10].

For the higher resolution models of subglacial till, the velocity at the top of the till layer will be varied based on the larger ice sheet model results. The basal topography will be based on CTX or HiRISE stereo DTMs of units superposed by banded terrain or simulated topography that mimics these units.

Results: Figure 2 shows the magnitude of horizontal velocity at the base of the ice sheet for one case, with low viscosity till (B=2×10^7 Pa s$^{1/3}$), surface temperature of 200 K, and heat flux of 30 mW/m^2. It shows that the region where velocity is highest only partially overlaps with the location of banded terrain, though the distribution varies with ice sheet geometry. For a higher viscosity till (B=10^9 Pa s$^{1/3}$), the velocity at the ice-till boundary is between 3 to 10 µm/yr, depending on the surface temperature and heat flux. The flow rate at the surface of the ice sheet is dominated by the ice deformation. For lower viscosity till (B= 2×10^7 Pa s$^{1/3}$), the velocity at the ice-till boundary is higher, between ~45 mm/yr to 60 mm/yr, with a relatively weaker dependence on surface temperature and heat flux. The flow rate at the surface of the ice sheet is dominated by the till deformation. Increasing the surface temperature from 200 K to 230 K increases the till velocity by 10 mm/yr. Doubling the heat flux from 30 to 60 mW/m^2 (at 200 K) increases the till velocity by 2 mm/yr.

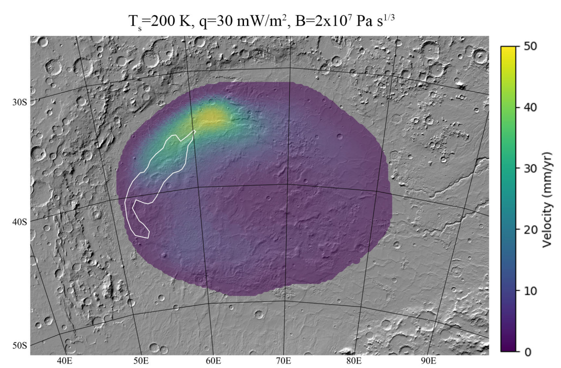

Figure 2: Top-down view of an ice sheet in Hellas basin, showing the horizontal velocity magnitude at the till surface after 600 years. White outline shows the banded terrain region. Maximum ice thickness at 68°E, 41°S is 1 km, surface temperature is 200 K, heat flux is 30 mW/m^2, B=2×10^7 Pa s$^{1/3}$, m=3, and d=1 mm.

Figure 3 shows the vertical displacement at the surface of the till layer for a case with low till viscosity, over a short time. With low viscosity, ridges form oriented approximately transverse to the ice flow direction (when the basal topography is a power law noise surface). After 10 years, the amplitude of vertical displacement at the surface is ~50 mm. At this rate, it would take ~2000 years to form ridges with the observed banded terrain relief of ~10 m, though this rate may change as ridge formation proceeds. Ridges are also seen, though less clearly, when using basal topography from a DTM. Ridges formed over longer wavelength topography are lower in amplitude. Thinner till leads to slightly higher amplitude deformation. Ridges do not form if the till drapes the basal topography with uniform thickness.

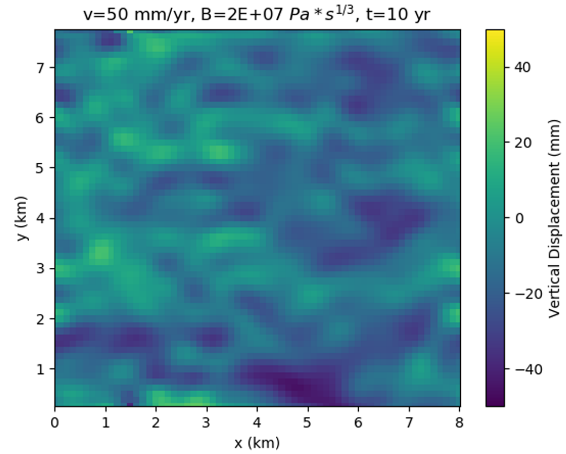

Figure 3: Top-down view of the till surface, showing the vertical component of displacement after 10 years. Velocity at the ice-till interface is 50 mm/yr, B=2×10^7 Pa s$^{1/3}$, m=3, and minimum till thickness is 30 m. Basal topography is a power-law noise surface with spectral exponent 1.8.

These results show that till deformation into ridges is possible, depending mainly on the velocity at the surface of the till. This velocity, determined from the ice sheet model, depends mostly on the till viscosity, though surface temperature and geothermal heat flux are also significant. The maximum basal velocities for a Hellas ice sheet overlap with the banded terrain. The location of fastest velocities can be affected by changing the shape of the ice sheet. Future work will further explore this parameter space and determine what conditions, if any, are suitable for explaining the observed banded terrain.

References: [1] Bernhardt H. et. al. (2019) *Icarus, 321*, 171-188. [2] Diot X. et. al. (2014) *Planetary & Space Science, 101*, 118-134. [3] Bernhardt H. et. al. (2016) *JGR, 121*, 714-738. [4] Diot X. et. al. (2015) *JGR, 120*, 2258-2276. [5] Stokes C. R. et al. (2016) *J. Glaciology 62*, 696-713. [6] Dunlop P. et al. (2008) *JGR, 113*, F03005. [7] Fowler A. C and Chapwanya M. (2014) *Proc. R. Soc. A, 470*, 20140185. [8] Goldsby D. L and Kohlstedt D. L. (2001) *JGR, 106*, 11017-11030. [9] Leysinger-Vieli G.J-M.C. and Gudmundsson G. H. (2010) *Cryosphere, 4*, 359-372. [10] Madeleine J. et. al. (2009) *Icarus, 203,* 390-405. [11] Fanale, F.P. (1976) *Icarus, 28,* 179-202. [12] Parro, L.M. et. al. (2017) *Sci. Rep., 7*, 45629. [13] Fastook, J. L. et. al. (2012) *Icarus, 219,* 25-40. [14] Porter, P. R. and Murray, T. (2001) *J. Glaciol., 47*, 167-175. [15] Dundas, C. M. et. al. (2014) *JGR Planets, 119*, 109-127. [16] Holt, J. W. et. al. (2008) *Science, 322,* 1235-1238.